# Influence of Al-Cr diffusion coating on low cycle fatigue behavior of cast nickel-base superalloy at 800 °C

Karel Obrtlík [1a], Simona Pospíšilová [2b], Martin Juliš [2c], Tomáš Podrábský [2d], and Tomáš Kruml [1e]

[1] Institute of Physics of Materials, Academy of Sciences of the Czech Republic, Žižkova 22, 616 62 Brno, Czech Republic

[2] Brno University of Technology, Faculty of Mechanical Engineering, Technická 2896/2, 616 69 Brno, Czech Republic

[a] obrtlik@ipm.cz, [b] pospisilova@fme.vutbr.cz, [c] julis@fme.vutbr.cz, [d] podrabsky@fme.vutbr.cz, [e] kruml@ipm.cz

**Keywords:** Low cycle fatigue, high temperature, diffusion coating, Inconel 713LC, cyclic hardening/softening curve, cyclic stress-strain curve, fatigue life curve, Knoop hardness.

**Abstract.** High temperature low cycle fatigue behavior of the cast nickel-based superalloy Inconel 713LC in as-received condition and coated with an Al-Cr diffusion layer have been investigated. The diffusion coating was deposited using the CVD out of pack technique. It was characterized and the hardness depth profile was measured. Fatigue tests were performed at 800 °C in air using cylindrical specimens. Cyclic hardening/softening curves, cyclic stress-strain curve and fatigue life curves were obtained. The detrimental effect of the surface treatment on the Manson-Coffin and the derived Wöhler curves is documented. Fracture surface and surface relief observations and examinations of specimen sections help to discuss the effect of the diffusion coating on the fatigue life.

## Introduction

Cast polycrystalline nickel base superalloy Inconel 713LC is a precipitation strengthened high temperature material. It is widely used for gas turbine blades and integral wheels of gas turbine engines whose critical parts are subjected to repeated elastic-plastic loading in aggressive environments at high temperatures. High temperature performance of cast superalloys can be improved with suitable protective diffusion coatings [1-3].

Fatigue behavior of untreated Inconel 713LC is reported scarcely [4-8]. The effect of diffusion coatings on the fatigue life of the superalloy is ambiguous [9-12]. The Manson-Coffin curve is shifted to higher fatigue lives while the derived Wöhler curve is moved to shorter lives in Al coated Inconel 713LC in comparison with the untreated material [9,10]. The beneficial effect of Al-Si diffusion coating on the fatigue life of Inconel 713LC at 800 °C both in the Manson-Coffin and Basquin representation is reported by Juliš et al. [11]. Si modified Al diffusion coating led to slight fatigue life decrease in the high amplitude domain of Inconel 713LC at 800 °C [12]. Besides, the microstructure and properties of the Al diffusion coating have been studied recently [9,13].

In this paper, the effect of Cr modified Al diffusion coating on the fatigue behavior of conventionally cast Inconel 713LC at 800 °C in air is studied. Experimental data on cyclic stress-strain response, fatigue life and surface layer characterization are presented. Fracture surface examinations and specimen sections and surface relief observations contribute to reveal the differences in the fatigue behavior of the treated and untreated superalloy.

## Experimental details

Polycrystalline superalloy Inconel 713LC was supplied by PBS Velká Bíteš, a.s. as conventionally cast rods. Its chemical composition (wt.%) is: 11.85 Cr, 5.80 Al, 4.54 Mo, 2.27 Nb, 0.72 Ti, 0.11 Zr, < 0.05 Co, < 0.05 Fe, < 0.05 Ta, < 0.05 Mn, < 0.05 Si, 0.05 Cu, 0.04 C, 0.015 B, 0.006 P, 0.004 S, Ni (balance). Polished and etched sections of the material reveal coarse grains with dendrites, carbides and shrinkage pores whose maximum size is 0.4 mm. An example of the structure can be seen in the optical micrograph of the section parallel to the rod axis in Fig. 1. The average dendritic grain size, found using the linear intercept method, was 2.3 mm. The microstructure consists of cuboidal $\gamma'$ precipitates embedded in $\gamma$ matrix.

Cylindrical specimens with button-ends had a gauge diameter and a gauge length of 6 and 15 mm, respectively. Their shape and dimensions are given elsewhere [14]. Specimens were machined parallel to the rod axis and their gauge length was mechanically ground. One half of specimens were surface treated with Al-Cr diffusion coating. Chemical vapor deposition technique was applied to provide Cr modified aluminizing of the specimen surface [15]. The coating was deposited in two steps: 1050 °C/5h and 950 °C/5h.

Both surface treated and untreated specimens were fatigued in a closed-loop electro-hydraulic testing system at total strain rate of $2 \times 10^{-3}$ $s^{-1}$ with fully reversed total strain cycle ($R_\varepsilon$ = -1) at 800 °C in air. Heating was provided by a three-zone resistance furnace and the temperature was monitored by three thermocouples. Strain was measured and controlled using a MTS extensometer 632.53F-14 with 12 mm base. Hysteresis loops for selected numbers of cycles were recorded in disk memory. Plastic strain amplitudes derived from the half of the loop width and stress amplitudes at half-life were evaluated.

Optical microscopy (OM) and scanning electron microscopy (SEM) Philips XL30 were used to study surface relief, fracture surfaces and polished sections of the gauge segments in both treated and untreated specimens. The micro-hardness was measured in LECO 400M-PC2 indentation tester equipped with the Knoop indenter using a load of 0.025 kgf (0.245 N). The chemical analysis of the diffusion coating was investigated with energy dispersion X-ray spectrometer EDAX built in SEM using spot and plane analysis.

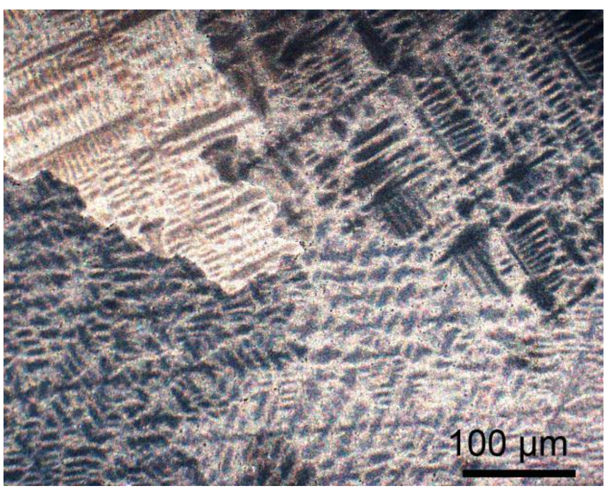


Fig. 1. Dendritic structure in the section parallel to the loading axis (OM).

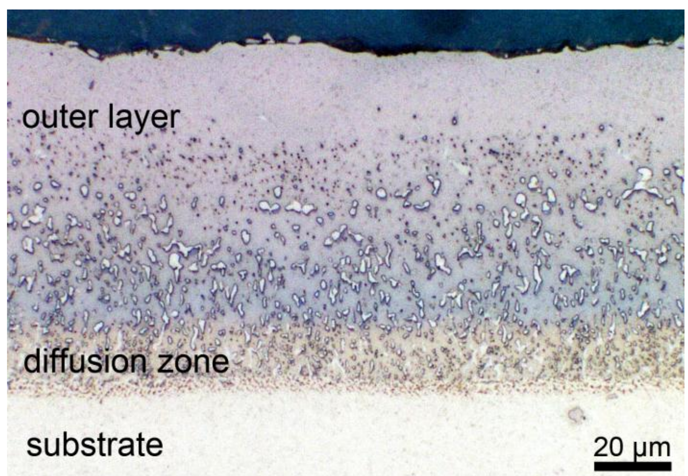


Fig. 2. Microstructure of a coated specimen in the section perpendicular to the specimen surface (OM).

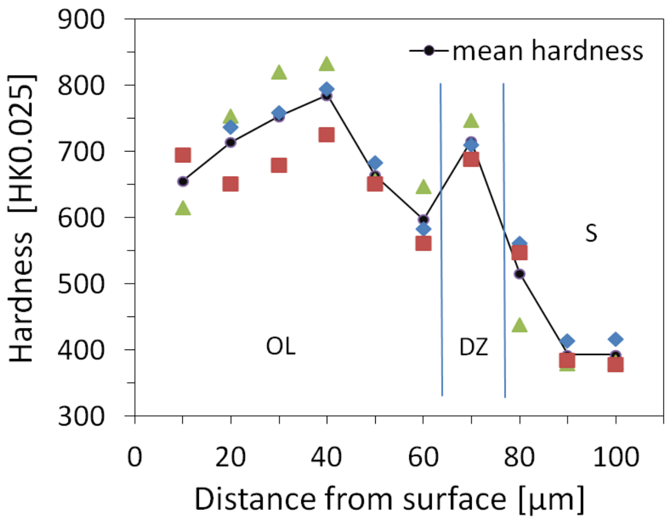


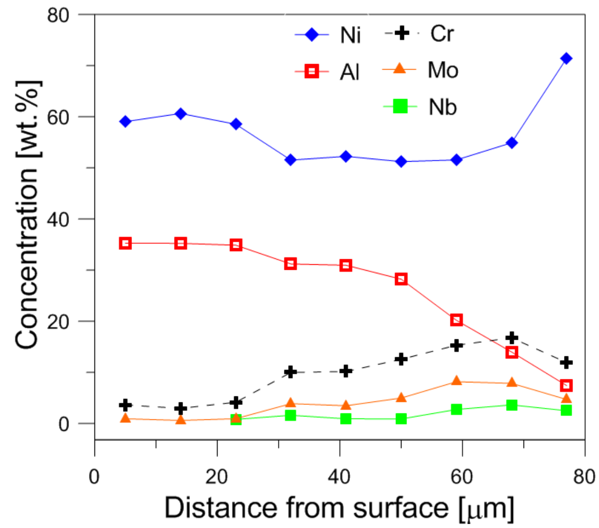


Fig. 3. Hardness versus distance from surface of a coated specimen measured in three different locations.

Fig. 4. Concentration profiles of major elements in the coating layer for a coated specimen.

**Results and discussion**

**Coating characterization.** Fig. 2 shows an OM image of a section perpendicular to the surface of a coated specimen. The Al-Cr diffusion coating consists of an outer layer (OL) and a diffusion zone (DZ). The total thickness of the coating ranges in the interval of 69 to 86 µm. The mean thickness of DZ is 14 µm. Cracks were not identified at the interface between the coating and substrate.
The concentration profiles of major elements in the coating measured by plane analysis are shown in Fig. 3. Individual phases in the coating were obtained through EDAX spot analysis. The outer layer of the coating is formed by the β NiAl phase with a number of small particles of Mo, Cr, and Nb based complex phases (including carbides) whose distribution and shape depend on a distance from the surface. Low density of particles occurs in the half of OL close to the surface. The diffusion zone consists of Ni-Al phases containing many Cr-Mo and Mo-Cr-Nb rich particles.

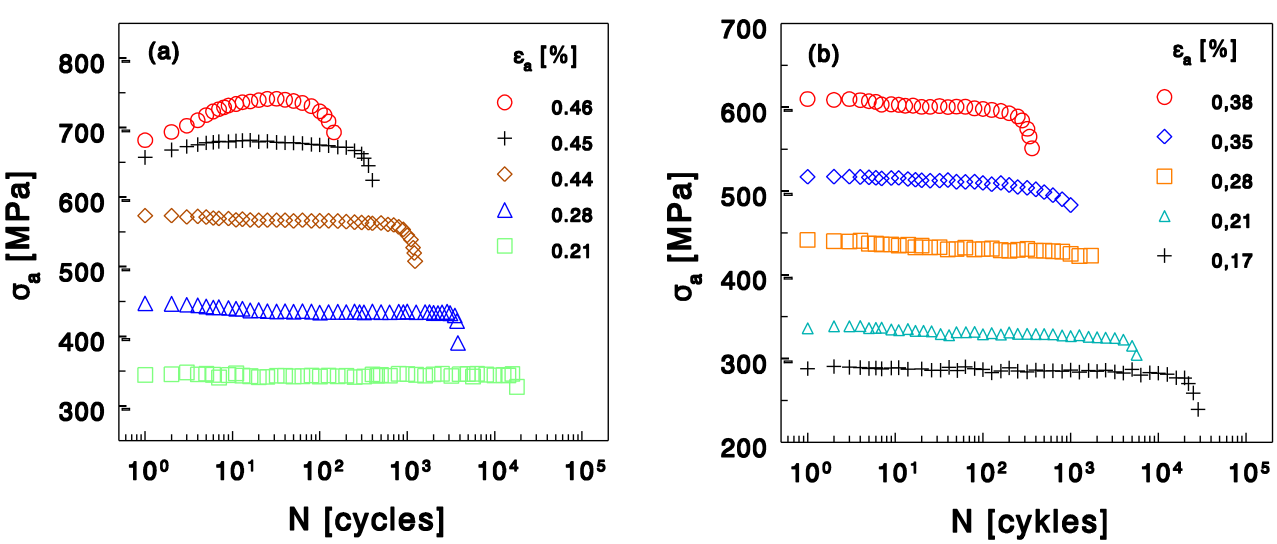


Fig. 5. Fatigue hardening/softening curves of the uncoated (a) and coated (b) Inconel 713LC.

Table 1. Parameters of cyclic stress-strain curve, Manson-Coffin curve and Basquin curve of uncoated and coated Inconel 713LC

| Inconel 713LC | K´ [MPa] | n´ | $\varepsilon_f'$ | c | $\sigma_f'$ [MPa] | b |
|---|---|---|---|---|---|---|
| uncoated | 3340 | 0.196 | 0.039 | - 0.78 | 1740 | - 0.150 |
| coated | 6500 | 0.261 | 0.0043 | - 0.61 | 1430 | - 0.147 |

Fig. 4 shows the micro-hardness depth profile measured in three different locations on the section perpendicular to the specimen surface. The Knoop hardness gradually increases from the surface to a maximum of 785 in the depth of 40 μm and then decreases up to the OL/DZ interface. The average Knoop hardness in the DZ and substrate is 716 and 427, respectively.

**Cyclic stress-strain response and fatigue life.** The stress amplitude $\sigma_a$ as a function of the number of cycles $N$ is shown in Fig. 5 for both coated and uncoated specimens cycled with different total strain amplitudes. In the uncoated material, the stable stress response is typical for low amplitudes while the initial hardening followed by saturation and softening is observed in the high amplitude domain - see Fig. 5a. Slow softening for all strain amplitudes can be seen in the coated superalloy – see Fig. 5b.

Fig. 6 shows cyclic stress-strain curves for both the uncoated and coated material. Experimental data were approximated by the power law

$$\log \sigma_a = \log K' + n' \log \varepsilon_{ap}. \tag{1}$$

and fatigue hardening coefficient K´ and fatigue hardening exponent n´ evaluated using regression analysis are shown in Table 1. Although the hardening exponents and the hardening coefficients differ appreciably experimental points of both materials are quite close to each other – see Fig. 6.

Fatigue life curves of the treated and untreated material are plotted in Fig. 7 and 8. Fig. 7 shows the plastic strain amplitude $\varepsilon_{ap}$ at half life versus the number of cycles to fracture $N_f$ in the bilogarithmic

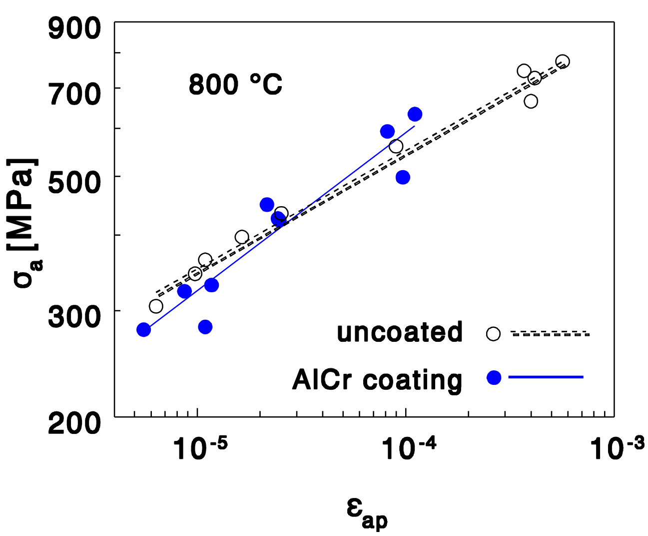


Fig. 6. Cyclic stress-strain curves of uncoated and coated Inconel 713LC.

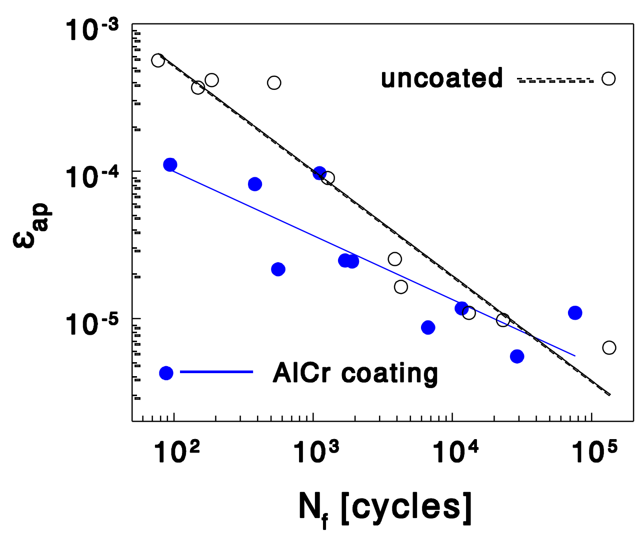


Fig. 7. Manson-Coffin curves of uncoated and coated Inconel 713LC.

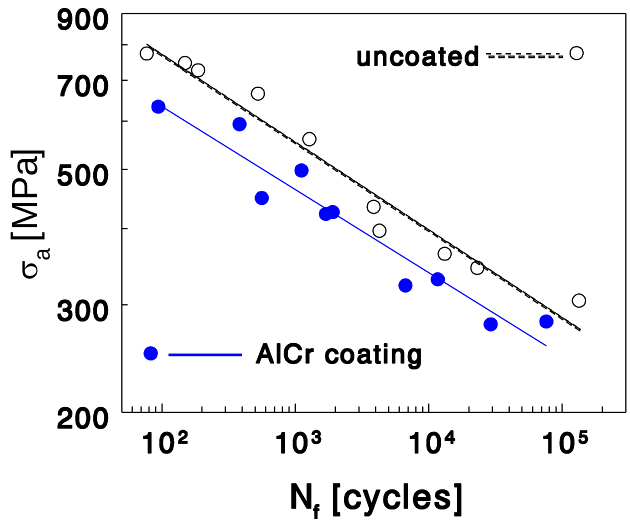


Fig. 8. Basquin plot for coated and uncoated Inconel 713LC.

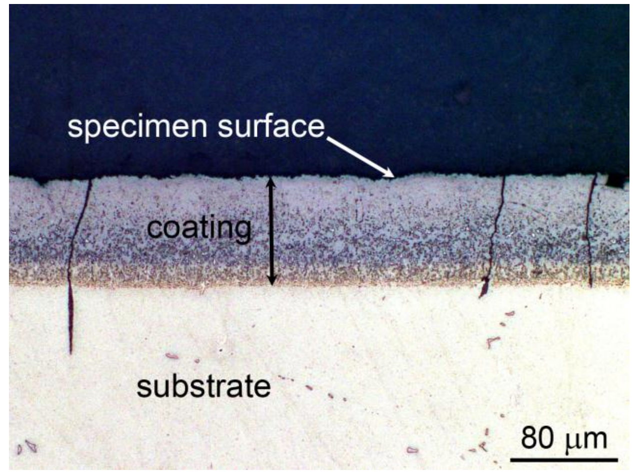


Fig. 9. Fatigue cracks growing from the surface to the substrate in a coated specimen (OM).

representation. Experimental data were fitted by the Manson-Coffin law

$$\log 2N_f = (1/c) \log \varepsilon_{ap} - (1/c) \log \varepsilon_f' \quad (2)$$

and the fatigue ductility coefficient, $\varepsilon_f'$, and the fatigue ductility exponent, c, evaluated using regression analysis are shown in Table 1. Fig. 7 shows a detrimental effect of the Al-Cr diffusion coating on the fatigue life in the high amplitude domain while for low amplitudes the fatigue life of both materials is similar. Fatigue life curves in the representation of the stress amplitude $\sigma_a$ at half-life versus the number of cycles to fracture $N_f$ are shown in Fig. 8. Experimental data were fitted by the Basquin law

$$\log 2N_f = (1/b) \log \sigma_a - (1/b) \log \sigma_f' \quad (3)$$

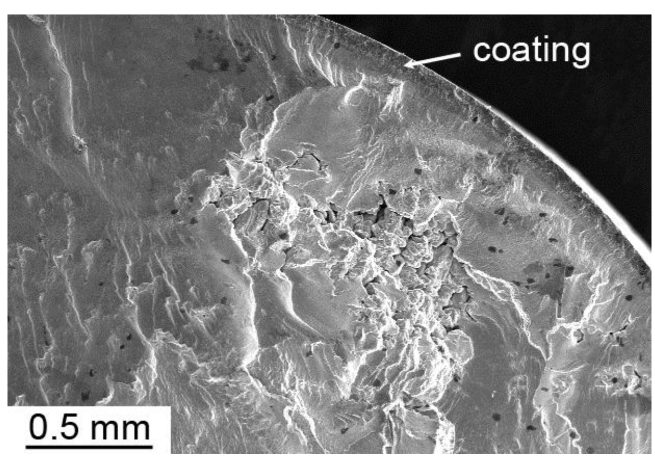


Fig. 10. SEM fractograph of a coated specimen with crack initiation caused by casting defect under the diffusion coating.

and the fatigue strength coefficient, $\sigma'_f$, and the fatigue strength exponent, b, are shown in Table 1 for both materials. It can be seen from Fig. 7 that the Basquin curve of coated specimens is shifted to lower fatigue lives for all stress amplitudes in comparison with that for uncoated Inconel 713LC.

**Specimen section observations and fractography.** An optical micrograph of the diamond and oxide polished section parallel to the loading axis of a coated specimen cycled to fracture ($\varepsilon_a$ = 0.19 %, $N_f$ = 76086 cycles) is shown in Fig. 9. Three fatigue cracks starting at the specimen surface can be seen in Fig. 9. They terminate at the coating/substrate interface (crack in the right) and in the substrate (the other cracks). Surface crack initiation was observed both in coated and uncoated material on sections parallel to the loading axis. The density of cracks increases with strain amplitude and is several times higher in coated specimens. In the high amplitude domain in the direction of the loading axis the typical density was 1.2 cracks/mm for uncoated material [9]. In coated Inconel 713LC, the density of surface cracks was 3.6 cracks/mm as early as at 1% $N_f$. Therefore, crack initiation is more homogeneous in the Al-Cr coated superalloy than in the untreated material.

Fracture surface observation reveals that casting defects present close to the specimen surface play decisive role in the principal crack initiation. Fig. 10 shows fracture surface of a coated specimen cycled to fracture with low strain amplitude ($\varepsilon_a$ = 0.17 %, $N_f$ = 29137). A casting defect present under the coating is apparent in Fig. 10. Stress concentration at the casting defect resulted in the main crack initiation.

Present results show that Al-Cr diffusion coating applied with CVD technique decreases the fatigue life of Inconel 713LC at 800 °C both in the Manson-Coffin and Basquin representation – see Fig. 7 and 8. Casting defects present close to the specimen surface result in the main crack nucleation both in coated and uncoated material. Besides, in the coated superalloy the comparative high density of surface layer cracks, originating already at the beginning of cycling, influences significantly the main crack initiation. Namely, the combination of surface cracks and casting defects under the surface layer accelerates the main crack formation. The cracked coating makes the incipient main crack longer which increases the stress and strain concentration at the crack tip and accelerates its propagation in comparison with the principal crack in uncoated material. Therefore, the fatigue life of surface treated Inconel 713LC is shorter than that of the untreated material.

## Conclusions

The experimental study of the effect of Al-Cr diffusion coating applied by the CVD out of pack technique on low cycle fatigue behavior of cast Inconel 713LC at 800 °C led to the following conclusions.

- The surface treatment has the detrimental effect on the fatigue life of the superalloy.
- Both the Manson-Coffin and Basquin curves of coated Inconel 713LC are shifted to lower fatigue life in comparison with those in uncoated superalloy.
- Surface crack initiation is more numerous in the coated material than in the uncoated one.

## Acknowledgment

The research was financially supported by the grants Nos. P107/11/2065 and P107/12/1922 of the Czech Science Foundation and by CEITEC – Central European Institute of Technology (CZ.1.05/1.1.00/02.0068) from European Regional Development Fund.

## References

[1] M. Durand-Charre: *The microstructure of superalloys* (Gordon and Breach Science Publishers, The Netherlands 1997).

[2] M.J. Donachie and S.J. Donachie: *Superalloys: a technical guide* (ASM International, USA 2002).

[3] S. Bose: *High temperature coatings* (Elsevier, The Netherlands 2007).

[4] K. Obrtlík, J. Man and J. Polák, in: *Proceedings of the Euromat 2001 conference*, AIM, Milano (2001), CD ROM No. 894.

[5] L. Kunz, P. Lukáš and R. Konečná: Int. J. Fatigue 32 (2010), p. 908.

[6] M. Petrenec, K. Obrtlík and J. Polák: Mater. Sci. Eng. A Vol. 400–401 (2005), p. 485.

[7] L. Kunz, P. Lukáš and R. Konečná: Eng. Fract. Mech. Vol. 77 (2010), p. 2008.

[8] K. Obrtlík, J. Man, M. Petrenec and J. Polák, in: *Fatigue 2002, Proceedings of the eighth international fatigue congress*, edited by A.F. Blom, EMAS, West Midlands, U.K. 2002, p. 963.

[9] K. Obrtlík, S. Pospíšilová, M. Juliš, T. Podrábský and J. Polák: Int. J. Fatigue Vol. 41 (2012), p. 101.

[10] K. Obrtlík, S. Pospíšilová, M. Juliš, T. Podrábský and J. Polák: Key Eng. Mater. Vol. 452-453 (2011), p. 265.

[11] M. Juliš, K. Obrtlík, S. Pospíšilová, T. Podrábský, and J. Polák: Procedia Eng. Vol. 2 (2010), p. 1983.

[12] K. Obrtlík, S. Pospíšilová, M. Juliš, T. Podrábský and J. Polák: Procedia Eng. Vol. 10 (2011), p. 1360.

[13] S. Pospíšilová, M. Juliš, K. Obrtlík, M. Kianicová, T. Podrábský and O. Dvořáček: Key Eng. Mater. Vol. 465 (2011), p. 282.

[14] K. Obrtlík, M. Petrenec, J. Man, J. Polák and K. Hrbáček: J. Mater. Sci. Vol. 44 (2009), p. 3305.

[15] M. Hetmańczyk, L. Swadźba and B. Mendala: J. Achiev. Mater. Manuf. Eng. Vol. 24 (2007), p. 372.